J. CHEM. SOC. DALTON TRANS. 1992

Synthesis and Site-selective Protonation of MoPt and WPt Bimetallic Complexes†

John Powell,* Jeffery F. Sawyer and Stuart J. Smith
Lash Miller Chemical Laboratories, University of Toronto, Toronto, Ontario M5S 1A1, Canada

---

The reaction of $[M(cp)(CO)_3(PPh_2H)]PF_6$ **1** (M = Mo or W, cp = η-C_5H_5) with $[Pt(C_2H_4)(PPh_3)_2]$ proceeds rapidly with a 1:2 (M:Pt) stoichiometry to give $[(OC)_2(cp)\overline{M(\mu\text{-}PPh_2)Pt}(CO)(PPh_3)]$ **4** and $[PtH(PPh_3)_3]PF_6$ **5**. However, using an initial 1:1 stoichiometry the final product is $[(OC)_2(cp)M(\mu\text{-}H)(\mu\text{-}PPh_2)Pt(PPh_3)_2]PF_6$ **8**. The mechanisms of these reactions are shown to involve deprotonation of **1** to give $[(OC)_3M(cp)(PPh_2)]$ **2** followed by reaction of the latter with $[Pt(C_2H_4)(PPh_3)_2]$ and subsequent transfer of CO from M to Pt to give **4**. Protonation of **4** with HBF_4 is metal (M) dependent and proceeds to give $[(OC)_2(cp)Mo(\mu\text{-}H)(\mu\text{-}PPh_2)Pt(CO)(PPh_3)]BF_4$ **12a** with M = Mo but for M = W the major product is $[(OC)_2H(cp)\overline{W(\mu\text{-}PPh_2)Pt}(CO)(PPh_3)]BF_4$ **13b**. Variable-temperature ^1H NMR studies show that the terminal hydride cation of **13b** is rapidly equilibrating with a small amount of the hydride-bridged isomeric cation $[(OC)_2(cp)W(\mu\text{-}H)(\mu\text{-}PPh_2)Pt(CO)(PPh_3)]^+$. Complex **4** reacts with PPh_3 (60 °C) and 1,2-bis(diphenylphosphino)ethane (dppe) at 20 °C to give $[(OC)_2(cp)\overline{M(\mu\text{-}PPh_2)Pt}(PPh_3)_2]$ **9** and $[(OC)_2(cp)\overline{M(\mu\text{-}PPh_2)Pt}(dppe)]$ **10**. On bubbling CO through a solution of **9** (20 °C) complex **4** is rapidly regenerated. Reaction of **4** with HCl gives $[(OC)_2(cp)M(\mu\text{-}H)(\mu\text{-}PPh_2)PtCl(PPh_3)]$ **15**. The molecular structure of $[(OC)_2(cp)\overline{W(\mu\text{-}PPh_2)Pt}(CO)(PPh_3)]$ **4b** has been determined by single-crystal X-ray diffraction.

Oxidative addition of the P–H bond of a secondary phosphine complex to platinum(0) complexes provides easy access to singly bridging μ-phosphido heterobimetallic hydrides of the type $L_xM(\mu\text{-}PR_2)PtHL_2$.[1–7] These complexes contain an 18-electron metal centre held by a μ-PR_2 group in close proximity to a 16-electron planar platinum(II) hydride. Because of the available stereochemical signposting (^1H, ^{13}C, ^{31}P, ^{195}Pt NMR spectroscopy, *etc.*) these systems are particularly suited for the study of cluster-assembly and -rearrangement processes[8,9] and for the study of ligand reactivities and 'co-operativity' effects in multimetallic systems. As an example of the latter the marked labilization (ease of displacement) of CO ligands on the 18-electron metal centre, M, in the complexes $[(OC)_5M(\mu\text{-}PR_2)PtH(PPh_3)_2]$ *vis-à-vis* monometallic analogues has been shown to be platinum assisted and involves a transfer of a CO ligand from M to Pt prior to displacement from the molecule.[1] The situation is similar, though slightly more complex, in the cationic RePt dimer $[(ON)(OC)(cp)Re(\mu\text{-}PR_2)PtH(PPh_3)_2]\ BPh_4$ (cp = η^5-cyclopentadienyl; R = Ph or C_6H_{11}).[2] Here loss of CO is base promoted and deprotonation (loss of the hydride ligand from the Pt as H^+) occurs prior to transfer of CO to Pt. In this paper we report an extension of these studies to the bimetallic complexes $[(OC)_2(cp)\overline{M(\mu\text{-}PPh_2)Pt}(CO)(PPh_3)]$ derived from the reaction of $[M(cp)(CO)_3(PPh_2H)]PF_6$ with $[Pt(C_2H_4)(PPh_3)_2]$. The protonation of the complexes $[(OC)_2(cp)\overline{M(\mu\text{-}PPh_2)Pt}(CO)(PPh_3)]$ is shown to exhibit an unusual M-dependent site selectivity, occurring at the metal–metal bond to give a bridged hydride cation for M = Mo whilst for M = W protonation occurs at tungsten to give a terminal hydrido cation. Some of this work has been the subject of a preliminary communication[10] and Braunstein and co-workers[11] have synthesised $[(OC)_2(cp)\overline{M\{\mu\text{-}P(C_6H_{11})_2\}Pt}(CO)\{P(C_6H_{11})_2H\}]$ [structural analogues of **4**] from the reaction of *trans*-$[Pt\{M(cp)(CO)_3\}_2(PhCN)_2]$ with 2 equivalents of $P(C_6H_{11})_2H$.

Results and Discussion

The cationic complexes $[M(cp)(CO)_3(PPh_2H)]PF_6$ (M = Mo **1a** or W **1b**) were prepared in 40–50% yields from $[M(cp)(CO)_3Cl]$[12] [equation (1)] following the general procedure of

$$[M(cp)(CO)_3Cl] + PPh_2H \xrightarrow{AlCl_3} \xrightarrow{[NH_4]PF_6} [M(cp)(CO)_3(PPh_2H)]PF_6 \quad (1)$$

1a M = Mo
1b M = W

Triechel *et al.*[13] whose previously reported preparation of **1a** resulted in a 22% yield. Spectroscopic data for **1** (Table 1) are fully consistent with the given structure and confirm the presence of a co-ordinated secondary phosphine [*e.g.* for **1a**, δ(PH) 7.46 (1:1 doublet), $^1J(^{31}P–^1H)$ 408 Hz]. The P–H bond of **1** is sufficiently acidic to undergo complete H/D exchange with $(CD_3)_2CO$ over a period of 24–36 h {20 °C, ^{31}P-{^1H}NMR monitoring; data for $[W(cp)(CO)_3(PPh_2D)]PF_6$ given in Table 1}. The complexes **1** are readily deprotonated by the addition of proton sponge [1,8-bis(dimethylamino)naphthalene] in CH_2Cl_2 solution (nitrogen atmosphere) to give the diphenylphosphide complexes $[M(cp)(CO)_3(PPh_2)]$ **2** [equation (2)].

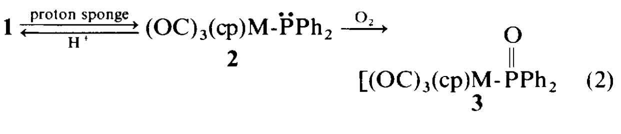

$$1 \underset{H^+}{\overset{\text{proton sponge}}{\rightleftharpoons}} \underset{\mathbf{2}}{(OC)_3(cp)M\text{-}\ddot{P}Ph_2} \xrightarrow{O_2} \underset{\mathbf{3}}{[(OC)_3(cp)M\text{-}\overset{\overset{\displaystyle O}{\|}}{P}Ph_2]} \quad (2)$$

The complexes **2** have been previously prepared from the reaction of PPh_2Cl with the anionic complexes $Na[M(cp)(CO)_3]$.[14] Solutions of $[M(cp)(CO)_3(PPh_2)]$ exhibit ν(CO) values (Table 1) that are shifted to lower wavenumber by *ca.* 50 cm^{-1} relative to $[M(cp)(CO)_3(PPh_2H)]PF_6$ consistent with removal of the positive charge. Addition of CF_3CO_2H to solutions of the diphenylphosphides **2** regenerates the ν(CO) of **1**. Solutions of **2** are very sensitive to oxidation reactions at the phosphorus atoms.[14] When exposed to oxygen the ν(CO) IR bands of **2** disappear within minutes and are replaced by new bands assignable to the species $[M(cp)(CO)_3\{P(O)Ph_2\}]$ **3** (Table 1). Although these species were not isolated, the

---

† *Supplementary data available:* see Instructions for Authors, *J. Chem. Soc., Dalton Trans.*, 1992, Issue 1, pp. xx–xxv.

Table 1 Infrared and ^{1}H and ^{31}P-{^{1}H}NMR data for complexes **1**–**3**

Complex	ν(CO)^a/cm^{-1}	δ(cp)^b	δ(P–H)	$J(^{31}P-^{1}H)$/Hz	δ(P)	$J(^{183}W-^{31}P)$/Hz
1a [Mo(cp)(CO)$_3$(PPh$_2$H)]PF$_6$	2063, 2003, 1975	5.72	7.46	408	10.3	
1b [W(cp)(CO)$_3$(PPh$_2$H)]PF$_6$	2057, 1989, 1962	5.81	7.63	417	−22.4	183
[W(cp)(CO)$_3$(PPh$_2$D)]PF$_6$		[$^1J(^{31}P-^{2}D)$ 64]			−24.8	181
2a [Mo(cp)(CO)$_3$(PPh$_2$)]	2009, 1926 (br)					
2b [W(cp)(CO)$_3$(PPh$_2$)]	2006, 1917 (br)					
3a [Mo(cp)(CO)$_3${P(O)Ph$_2$}]	2033, 1963, 1942					
3b [W(cp)(CO)$_3${P(O)Ph$_2$}]	2029, 1952, 1932					

^{a} In CH$_2$Cl$_2$ solution. ^{b} In CD$_2$Cl$_2$ solution.

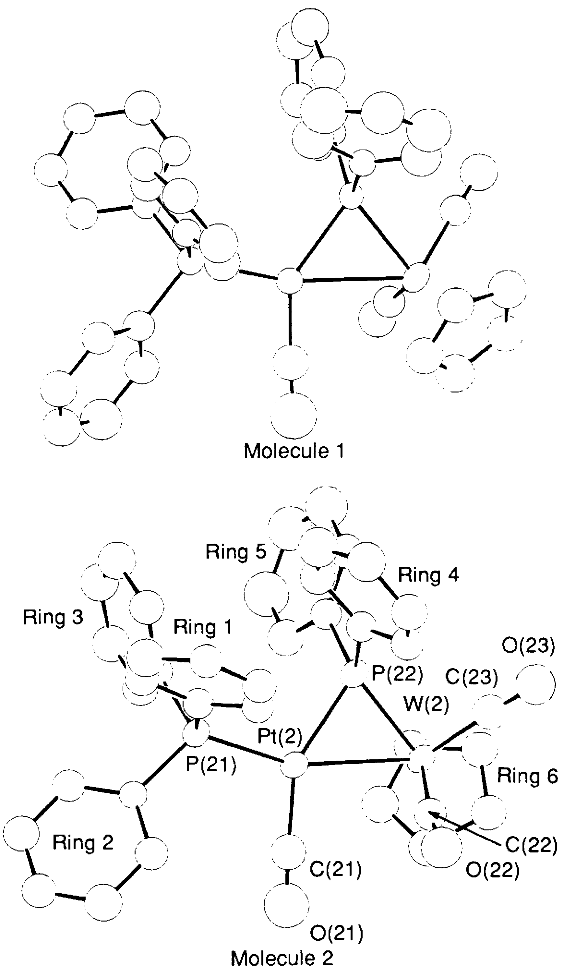

Fig. 1 The structure and labelling scheme for the two independent molecules of [(OC)$_2$(cp)W(μ-PPh$_2$)Pt(CO)(PPh$_3$)] **4b**

oxidation of **2** to **3** is comparable to the reaction of **2** with S$_8$ to give [M(cp)(CO)$_3${P(S)Ph$_2$}][14] and the O$_2$ oxidation of [Re(cp)(CO)(NO)(PPh$_2$)] to give [Re(cp)(CO)(NO)-{P(O)Ph$_2$}].[15]

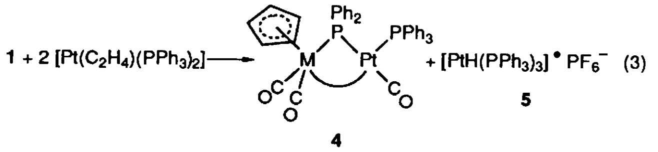

(3)

4 **5**

Reaction of [M(cp)(CO)$_3$(PPh$_2$H)]PF$_6$ *with* [Pt(C$_2$H$_4$)-(PPh$_3$)$_2$].—Infrared monitoring of the ν(CO) region in CH$_2$Cl$_2$ solution showed that the complexes [M(cp)(CO)$_3$(PPh$_2$H)]PF$_6$ **1** react with [Pt(C$_2$H$_4$)(PPh$_3$)$_2$] in 1:2 stoichiometry *via* a short-lived intermediate to give the neutral bimetallic complexes [(OC)$_2$(cp)M(μ-PPh$_2$)Pt(CO)(PPh$_3$)] (M = Mo **4a** or W **4b**) and the known cationic platinum hydride [PtH(PPh$_3$)$_3$]-PF$_6$ **5**[16,17] [equation (3)]. These products are readily crystallized from solution. The molecular structure of [(OC)$_2$(cp)-W(μ-PPh$_2$)Pt(CO)(PPh$_3$)] **4b** as determined by single-crystal X-ray diffraction is shown in Fig. 1. The solution IR spectrum of **4b** (in CH$_2$Cl$_2$, Table 2) exhibits two ν(CO) at 1904 and 1824 cm^{-1} assignable to the tungsten carbonyls and one at 2019 cm^{-1} assignable to the CO on Pt. The relative intensities $I(1904)/I(1824) = I(\text{sym.})/I(\text{asym.}) = 1.50$ correspond to a 'predicted' (OC)W(CO) angle of 78°[18,19] (84° from X-ray structural data). The ^{31}P-{^{1}H} NMR data for [(OC)$_2$(cp)M(μ-PPh$_2$)Pt-(CO)(PPh$_3$)] **4** (Table 3) are also consistent with the structure shown. The downfield shift of the μ-PPh$_2$ ligand[1–9] [δ(P$_\mu$) 140 for **4b**] and the coupling to ^{183}W and ^{195}Pt [$^1J(^{183}W-^{31}P_\mu)$ = 317; $^1J(^{195}Pt-^{31}P_\mu)$ = 2528 Hz for **4b**] are consistent with a metal–metal bonded 'W(μ-PPh$_2$)Pt' unit, and the small $^2J(^{31}P-^{31}P_\mu)$ 19 Hz is consistent with a *cis* arrangement of P-donor ligands on Pt. The cationic hydride [PtH(PPh$_3$)$_3$]PF$_6$ is readily identified by its characteristic ^{1}H and ^{31}P-{^{1}H} NMR spectra.[17]

Infrared monitoring of the reaction of [M(cp)(CO)$_3$-(PPh$_2$H)]PF$_6$ **1** with [Pt(C$_2$H$_4$)(PPh$_3$)$_2$] within minutes of mixing reveals the presence of a short-lived intermediate with ν(CO) at 2030, 1956 and 1934 cm^{-1} (M = W). The lower values *vis-à-vis* cation **1** suggest removal of the positive charge from the tungsten centre. The ν(CO) of this intermediate are at higher wavenumbers than those of [M(cp)(CO)$_3$(PPh$_2$)] **2** and very similar to those observed for [M(cp)(CO)$_3${P(O)Ph$_2$}] **3** (Table 1). On the basis of the IR evidence we suggest that the short-lived intermediate is either the neutral complex [(OC)$_3$(cp)M(μ-PPh$_2$)Pt(PPh$_3$)$_2$] **6** or the cationic bimetallic [(OC)$_3$(cp)M-(μ-PPh$_2$)PtH(PPh$_3$)$_2$]$^+$ **7** (see Scheme 2).

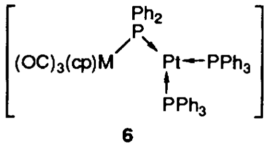

6

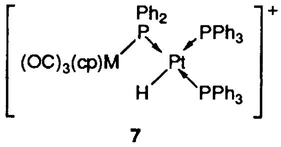

7

When [M(cp)(CO)$_3$(PPh$_2$H)]PF$_6$ **1** is treated with a molar equivalent of [Pt(C$_2$H$_4$)(PPh$_3$)$_2$] the reaction proceeds quickly (*ca.* 10 min) to give a solution containing equimolar amounts of **1**, **4** and **5** {^{1}H, ^{31}P-{^{1}H} NMR and IR monitoring). *On further standing* the ν(CO) absorptions of **1** and **4** (IR monitoring) decrease and two new absorptions grow in [ν(CO) 1964 and 1891 cm^{-1} for M = W]. This reaction is complete in *ca.* 16 h for M = W and *ca.* 4 h for M = Mo. The new products are

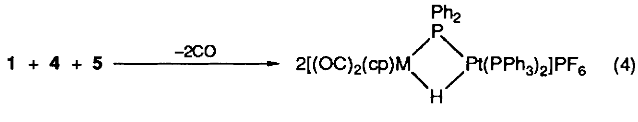

(4)

Table 2 Infrared[a] and ^1H NMR data[b] of the MoPt and WPt dimeric complexes (P_a is *trans* to μ-H). See equations and Scheme 1 for structures

Complex	δ(cp)	δ(H)	$^1J(^{195}Pt-^1H)$	$^1J(^{183}W-^1H)$	$^2J(^{31}P-^1H)$	$^2J(^{31}P_b-^1H)$	$^2J(^{31}P_a-^1H)$	IR (cm^{-1}) ν(CO)	IR (cm^{-1}) ν(Pt–CO)
4a $[(OC)_2(cp)\overline{Mo(\mu\text{-}PPh_2)Pt}(CO)(PPh_3)]$	5.10							1911, 1834	2018
4b $[(OC)_2(cp)\overline{W(\mu\text{-}PPh_2)Pt}(CO)(PPh_3)]$	5.17							1904, 1824	2019
8a $[(OC)_2(cp)Mo(\mu\text{-}H)(\mu\text{-}PPh_2)Pt(PPh_3)_2]PF_6$	4.55	−9.50	499	—	24	18	78	1973, 1905	
8b $[(OC)_2(cp)W(\mu\text{-}H)(\mu\text{-}PPh_2)Pt(PPh_3)_2]PF_6$	4.63	−9.34	494	42	20	18	74	1964, 1891	—
9a $[(CO)_2(cp)\overline{Mo(\mu\text{-}PPh_2)Pt}(PPh_3)_2]$	4.47							1892, 1808	—
9b $[(OC)_2(cp)\overline{W(\mu\text{-}PPh_2)Pt}(PPh_3)_2]$	4.47							1886, 1797	—
10a $[(OC)_2(cp)\overline{Mo(\mu\text{-}PPh_2)Pt}(dppe)]$	4.49							1884, 1804	—
10b $[(OC)_2(cp)\overline{W(\mu\text{-}PPh_2)Pt}(dppe)]$	4.48							1877, 1796	—
11a $[(OC)_2(cp)Mo(\mu\text{-}H)(\mu\text{-}PPh_2)Pt(dppe)]BF_4$	4.71	−7.71	544	—	22	8	73	1972, 1905	—
11b $[(OC)_2(cp)W(\mu\text{-}H)(\mu\text{-}PPh_2)Pt(dppe)]BF_4$	4.80	−7.98	521	44	19	9	70	1964, 1891	
12a $[(OC)_2(cp)Mo(\mu\text{-}H)(\mu\text{-}PPh_2)Pt(CO)(PPh_3)]BF_4$[c]	5.32	−8.87	520	—	29	—	65	1991, 1928	2102
13b $[(OC)_2H(cp)\overline{W(\mu\text{-}PPh_2)Pt}(CO)(PPh_3)]BF_4$[c]	5.46	−5.04	85	42	46	—	7.5	2010, 1961	2083
14a $[(OC)_2(cp)Mo(\mu\text{-}H)(\mu\text{-}PPh_2)Pt(CO)(PPh_3]BF_4$[d]	4.84	−9.17	559	—	13	20	—	1991, 1930	2102
14b $[(OC)_2(cp)W(\mu\text{-}H)(\mu\text{-}PPh_2)Pt(CO)(PPh_3)]BF_4$[d]	4.94	−9.15	559	42	14	16	—	1984, 1918	2099
15a $[(OC)_2(cp)Mo(\mu\text{-}H)(\mu\text{-}PPh_2)PtCl(PPh_3)]$[c]	5.07	−8.40	445	—	27	—	79	1959, 1887	
15b $[(OC)_2(cp)W(\mu\text{-}H)(\mu\text{-}PPh_2)PtCl(PPh_3)]$[c]	5.19	−8.35	440	47	25	—	76	1950, 1874	
16a $[(OC)_2(cp)Mo(\mu\text{-}H)(\mu\text{-}PPh_2)PtCl(PPh_3)]$[d]	4.68	−15.6	684	—	10	19	—	1959, 1887	
16b $[(OC)_2(cp)W(\mu\text{-}H)(\mu\text{-}PPh_2)PtCl(PPh_3)]$[d]	4.75	−15.4	678	46	10	17	—	1950, 1874	

[a] In CH_2Cl_2 solution. [b] In CD_2Cl_2 solution, *J* in Hz. [c] PPh_3 *cis* to μ-PPh_2. [d] PPh_3 *trans* to μ-PPh_2.

Table 3 $^{31}P-\{^1H\}$ NMR data (*J* in Hz) for MoPt and WPt dimeric complexes (P_a *trans* to μ-H). See equations and Scheme 1 for structures

Complex	$\delta(P_\mu)$	$\delta(P_a)$	$\delta(P_b)$	$J(^{195}Pt-^{31}P_\mu)$	$J(^{195}Pt-^{31}P_a)$	$J(^{195}Pt-^{31}P_b)$	$J(^{31}P_\mu-^{31}P_a)$	$J(^{31}P_\mu-^{31}P_b)$	$J(^{31}P_a-^{31}P_b)$	$J(^{183}W-^{31}P_\mu)$
4a	177	30	—	2742	3332	—	11	—	—	—
4b	140	21	—	2528	3271	—	19	—	—	317
8a	184	20	11	1889	3806	2478	8	223	23	—
8b	147	12	11	1765	3942	2481	0	218	23	217
9a	187	28	30	2597	3374	3271	10	219	3.4	—
9b	150	24	26	2403	3296	3266	17	221	0	337
11a	171	53	53	1909	3505	2420	2	228	6.1	—
11b	133	47	26	1803	3607	2420	0	224	7.6	190
12a	169	20	—	2202	3635	—	7	—	—	—
13b	119	26	—	2272	3500	—	12	—	—	202
14a	195	—	18	1365	—	2437	—	168	—	—
14b	158	—	18	1277	—	2437	—	164	—	247
15a	167	34	—	3048	4192	—	2	—	—	—
15b	132	31	—	2908	4338	—	0	—	—	226
16a	173	—	25	1899	—	2799	—	303	—	—
16b	136	—	27	1791	—	2714	—	294	—	226

the cationic μ-hydrido complexes $[(OC)_2(cp)M(\mu\text{-}H)(\mu\text{-}PPh_2)Pt(PPh_3)_2]PF_6$ **8** [equation (4)]. Complexes **8** are readily isolated and structurally characterized. The relative ν(CO) intensities *I*(1964)/*I*(1891) = 1.60 for **8b** correspond to a calculated (OC)W(CO) angle of 77°.[18,19] The ^1H NMR spectrum of $[(OC)_2(cp)W(\mu\text{-}H)(\mu\text{-}PPh_2)Pt(PPh_3)_2]PF_6$ **8b** (see Fig. 2 and Table 2) shows a multiline pattern centred at δ −9.34 assignable to a hydride ligand coupled to ^{183}W, ^{195}Pt and three ^{31}P nuclei with $J(^{195}Pt-^1H)$ 494 Hz and $J[^{31}P$ (*trans* to H)–$^1H]$ 74 Hz consistent with the hydride-bridged structure shown.[1,20] Whilst the ^{195}Pt satellite resonance patterns are first order, second-order coupling effects are observed in the main pattern due to the similarity in the ^{31}P chemical shifts of the two PPh_3 ligands (see Fig. 2). This kind of effect has been previously

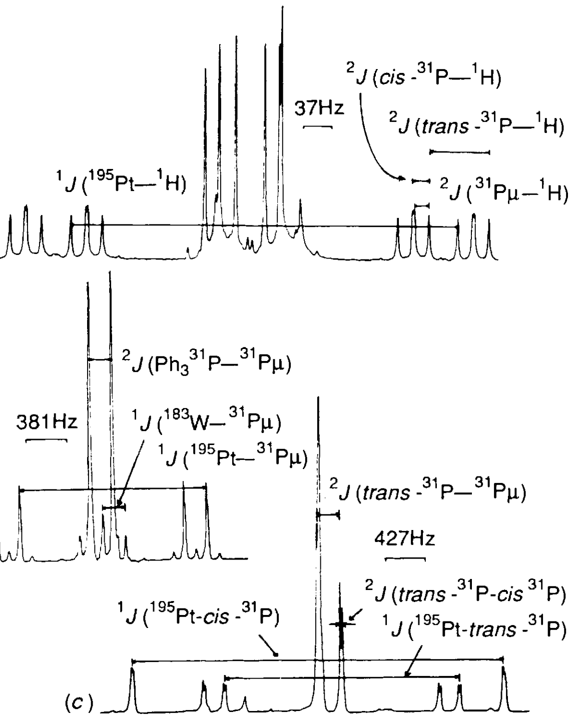

Fig. 2 Proton NMR spectrum (*a*) of $[(OC)_2(cp)W(\mu\text{-}H)(\mu\text{-}PPh_2)\text{-}Pt(PPh_3)_2]PF_6$ **8b** in the hydrido region (CD_2Cl_2 solution), and the $^{31}P\text{-}\{^1H\}$ NMR spectrum of **8b** in the phosphido (P_μ) (*b*) and PPh_3 regions (*c*). Note the partial overlap of PPh_3 resonances and the resulting effect on the ^1H NMR spectrum[12]

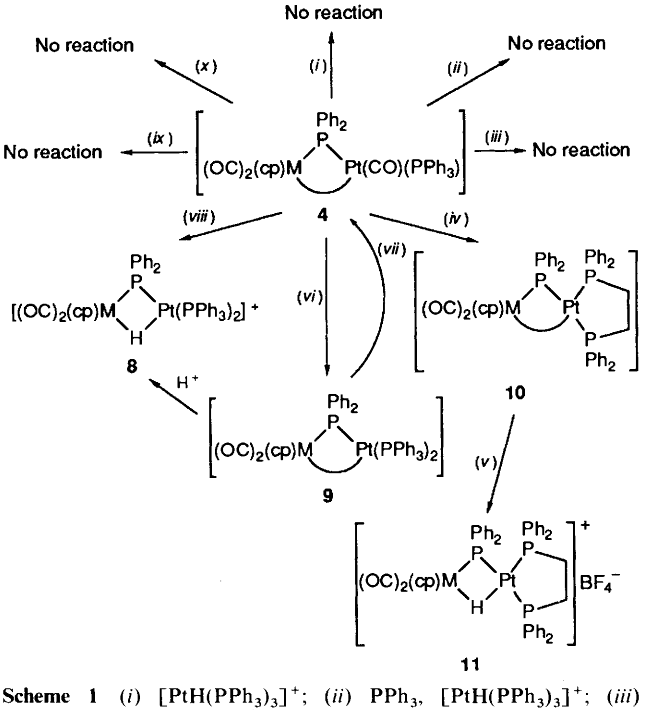

Scheme 1 (*i*) $[PtH(PPh_3)_3]^+$; (*ii*) PPh_3, $[PtH(PPh_3)_3]^+$; (*iii*) CF_3CO_2H, $[PtH(PPh_3)_3]^+$; (*iv*) dppe, 20 °C; (*v*) HBF_4; (*vi*) PPh_3, reflux in C_6H_6; (*vii*) CO, 20 °C; (*viii*) CF_3CO_2H, PPh_3, 20 °C, rapid; (*ix*) PPh_3, 20 °C; (*x*) CF_3CO_2H

observed and commented on for a series of cations of the type $[PtH(PR_3)_3]^+$.[17]

Reaction of $[(OC)_2(cp)M(\mu\text{-}PPh_2)Pt(CO)(PPh_3)]$ **4** *with P-Donor Ligands*.—In order to ascertain the likely mechanism for the formation of $[(OC)_2(cp)M(\mu\text{-}H)(\mu\text{-}PPh_2)Pt(PPh_3)_2]\text{-}PF_6$ **8** from an equimolar mixture of compounds **1**, **4** and **5** [equation (4)] the reaction of **4** with a range of reagents was investigated (Scheme 1). Compounds **4** did not react with PPh_3 at room temperature. On refluxing an equimolar mixture of **4** and PPh_3 in benzene, CO was lost and the complex $[(OC)_2(cp)\text{-}M(\mu\text{-}PPh_2)Pt(PPh_3)_2]$ **9** could readily be isolated and characterized (Tables 2 and 3). On bubbling CO through a CH_2Cl_2 solution of **9** (*ca.* 20 °C) the PPh_3 ligand *trans* to the phosphido bridge was rapidly displaced and **4** regenerated. Addition of a molar equivalent of 1,2-bis(diphenylphosphino)-ethane (dppe) to **4** gave $[(OC)_2(cp)M(\mu\text{-}PPh_2)Pt(dppe)]$ **10**. This reaction was relatively fast at room temperature and probably proceeds by initial displacement of PPh_3 by dppe followed by ring closing and loss of CO. The complexes **9** and **10** are readily protonated (CF_3CO_2H or HBF_4) to give the μ-hydrido cations $[(OC)_2(cp)M(\mu\text{-}H)(\mu\text{-}PPh_2)Pt(PPh_3)_2]^+$ and $[(OC)_2(cp)M(\mu\text{-}H)(\mu\text{-}PPh_2)Pt(dppe)]^+$ respectively *e.g.* **11**, Scheme 1). Whilst **4** did not react with CF_3CO_2H, the addition of both CF_3CO_2H and PPh_3 (20 °C) resulted in rapid formation of the cations $[(OC)_2(cp)M(\mu\text{-}H)(\mu\text{-}PPh_2)Pt\text{-}(PPh_3)_2]^+$ **8**. These observations point to protonation of **4** occurring prior to the displacement of CO from Pt by the PPh_3 ligand (N.B. PPh_3 alone does not displace CO from **4** at room temperature). No reaction occurred when either $[PtH\text{-}(PPh_3)_3]^+$, $[PtH(PPh_3)_3]^+\text{-}PPh_3$ or $[PtH(PPh_3)_3]^+\text{-}CF_3CO_2H$ were added to solutions of **4**.

Reaction of Compounds **4** *with* $HBF_4\cdot OEt_2$[12] *and* HCl.—The molybdenum complex **4a** is readily protonated by the addition of a molar equivalent of the strong acid $HBF_4\cdot OEt_2$ (added as a CH_2Cl_2 solution). Proton and $^{31}P\text{-}\{^1H\}$ NMR monitoring of the resultant solution indicated that the protonation product was $[(OC)_2(cp)Mo(\mu\text{-}H)(\mu\text{-}PPh_2)Pt(CO)(PPh_3)]BF_4$ **12a** [equation (5)]. The '(μ-H)(μ-PPh₂)' structure is readily confirmed by NMR spectroscopy (Tables 2 and 3) as is the *cis* arrangement of the two P-donor ligands on Pt [*e.g.* $^1J(^{195}Pt\text{-}^1H_\mu)$ = 520 Hz, $\delta(P_\mu)$ 169, $^2J(^{31}P\text{-}^{31}P_\mu)$ = 7.2 Hz, *etc.*]. In marked contrast to the protonation of **4a**, the isostructural WPt dimer **4b** reacts with a molar equivalent of HBF_4 to give the terminal hydrido cation $[(OC)_2(cp)H\text{-}W(\mu\text{-}PPh_2)Pt(CO)(PPh_3]BF_4$ **13b**. Support for this structure comes from the high-field ^1H NMR spectrum (Table 2 and Fig. 3). Of particular significance are the very small spin–spin couplings of the hydride with ^{195}Pt (85 Hz, 20 °C) and with the ^{31}P of the PPh_3 bonded to Pt (7.5 Hz; confirmed by recording the proton-coupled ^{31}P NMR spectrum).[2,4] The small $^2J(^{31}P\text{-}^{31}P_\mu)$ 11.6 Hz implies a *cis* arrangement of P-donor ligands. Other terminal hydrido 'MPt' bimetallic structural analogues of **13b** that have been structurally characterized by X-ray diffraction are $[(ON)H(cp)Re\{\mu\text{-}P(C_6H_{11})_2\}Pt(PPh_3)_2]BF_4$[2] and $[(OC)_3HFe(\mu\text{-}PPh_2)Pt(PPh_3)_2]$.[4] On standing both **12a** and

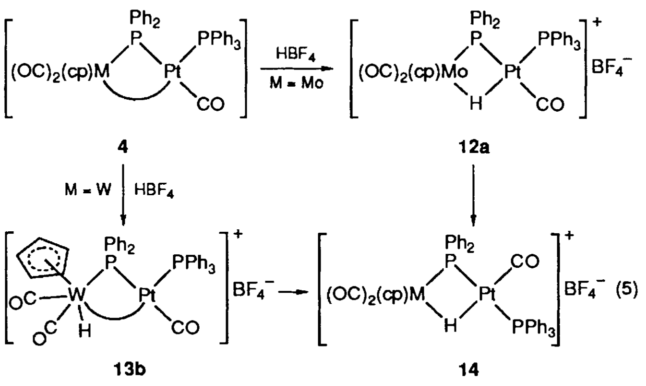

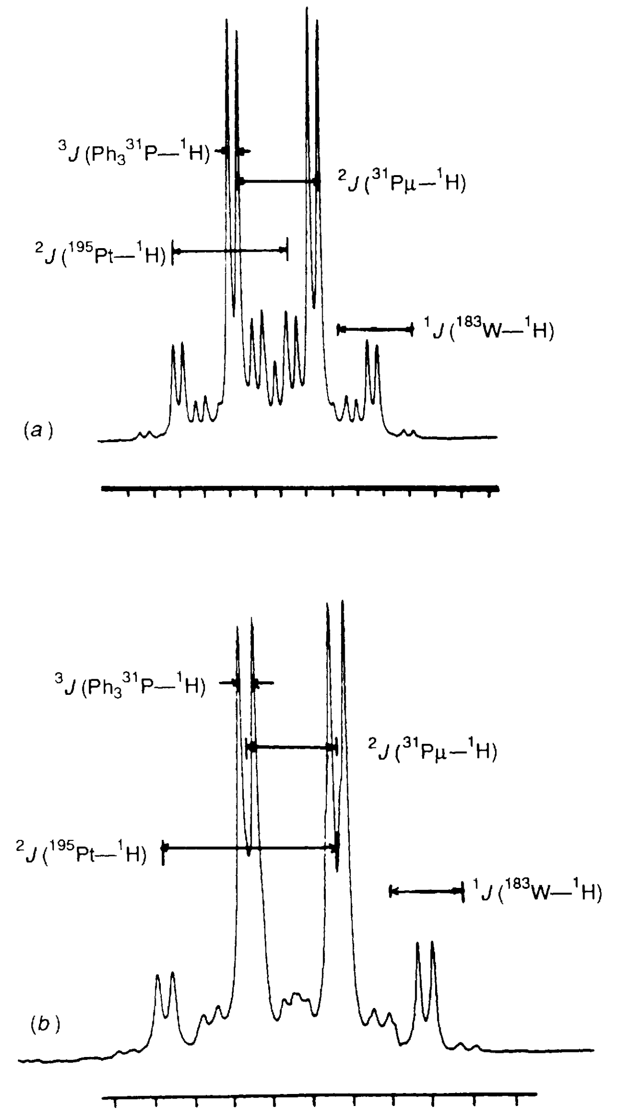

Fig. 3 Proton NMR spectrum, hydrido region (CD_2Cl_2 solution) for $[(OC)_2H(cp)W(\mu\text{-}PPh_2)Pt(CO)(PPh_3)]BF_4$ **13b** at −40 (*a*) and +20 °C (*b*)

13b undergo a slow *cis-to-trans* isomerization at Pt to give the hydrido-bridged cations $[(OC)_2(cp)M(\mu\text{-}H)(\mu\text{-}PPh_2)Pt(CO)(PPh_3)]BF_4$ **14** (PPh_3 *trans* to P_μ) [equation (5)]. The presence of a μ-H and *trans* arrangement of P-donor ligands in **14** is readily confirmed by NMR spectroscopy (see Tables 2 and 3 for NMR and IR data). The cations **12a**, **13b** and **14** react 'instantly' with PPh_3, with evolution of CO, to give $[(OC)_2(cp)M(\mu\text{-}H)(\mu\text{-}PPh_2)Pt(PPh_3)_2]BF_4$ {same cation as **8** [equation (4)]}.

The addition of a molar equivalent of HCl (benzene solution) to $[(OC)_2(cp)M(\mu\text{-}PPh_2)Pt(CO)(PPh_3)]$ occurs according to equation (6) to give $[(OC)_2(cp)M(\mu\text{-}H)(\mu\text{-}PPh_2)PtCl(PPh_3)]$ **15** (PPh_3 *cis* to P_μ) as the kinetic product. The complexes **15** are readily characterized by IR and NMR spectroscopy (Tables 2 and 3). Upon standing in solution (room temperature), **15** slowly isomerizes to the *trans* isomer $[(OC)_2(cp)M(\mu\text{-}H)(\mu\text{-}PPh_2)PtCl(PPh_3)]$ **16** (PPh_3 *trans* to P_μ). For M = Mo the rearrangement proceeds over a period of a few days whilst for M = W the rearrangement is only 50% complete after 3 weeks. The formation of **15** as the kinetic product suggests that reaction of **4** with HCl is similar to that with $CF_3CO_2H\text{–}PPh_3$ (see above) and proceeds *via* initial protonation of **4** to give the cations of **12**/**13b** followed by rapid displacement of CO by Cl^-. The sensitivity of the rate of the **15** to **16** rearrangement

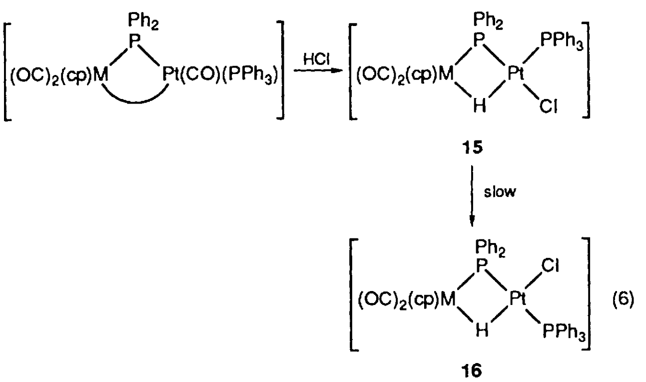

[equation (6)] to the nature of M suggests considerable perturbation of a metal–ligand(s) bond(s)[21] but the mechanism is not readily defined.

Mechanism of Formation of $[(OC)_2(cp)M(\mu\text{-}PPh_2)Pt(CO)(PPh_3)]$, $[PtH(PPh_3)_3]PF_6$ *and* $[(OC)_2(cp)M(\mu\text{-}H)(\mu\text{-}PPh_2)Pt(PPh_3)_2]PF_6$ [*equations* (3) *and* (4)].—Based on the above experimental observations the reaction of $[M(cp)(CO)_3(PPh_2H)]PF_6$ **1** with 2 equivalents of $[Pt(C_2H_4)(PPh_3)_2]$ is postulated to occur *via* the reaction pathways outlined in Scheme 2. Step (i) is the protonation of $[Pt(C_2H_4)(PPh_3)_2]$ by complex **1** resulting in formation of the metallaphosphine $[M(cp)(CO)_3(PPh_2)]$ **2** and the cation $[PtH(C_2H_4)(PPh_3)_2]^+$. Complex **2** then reacts with another molecule of $[Pt(C_2H_4)(PPh_3)_2]$, step (ii), displacing ethylene to form $[(OC)_3(cp)M(\mu\text{-}PPh_2)Pt(PPh_3)_2]$ **6**, the possible 'short-lived intermediate'. Complex **6** then rearranges, step (iii), to form $[(OC)_2(cp)M(\mu\text{-}PPh_2)Pt(CO)(PPh_3)]$ **4** presumably *via* triphenylphosphine dissociation and carbonyl ligand migration *via* the μ-CO complex $[(OC)_2(cp)M(\mu\text{-}CO)(\mu\text{-}PPh_2)Pt(PPh_3)_2]$ **17**. The dissociated triphenylphosphine from step (iii) is consumed by reaction with the cation $[PtH(C_2H_4)(PPh_3)_2]^+$ to form $[PtH(PPh_3)_3]^+$ [step (iv)] or with $[Pt(C_2H_4)(PPh_3)_2]$ to form $[Pt(PPh_3)_3]$. The $[Pt(PPh_3)_3]$ can function as a base to deprotonate **1** to give **2** and **5** [steps (v) and (vi)].

As discussed above a 1:1 reaction mixture of $[M(cp)(CO)_3(PPh_2H)]PF_6$ **1** and $[Pt(C_2H_4)(PPh_3)_2]$, in CH_2Cl_2 at 25 °C, proceeds *rapidly* to give an equimolar mixture of **1**, $[(OC)_2(cp)M(\mu\text{-}PPh_2)Pt(CO)(PPh_3)]$ **4** and $[PtH(PPh_3)_3]PF_6$ **5** which then *slowly* converts, with loss of carbon monoxide, into $[(OC)_2(cp)M(\mu\text{-}H)(\mu\text{-}PPh_2)Pt(PPh_3)_2]PF_6$ **8**. It is postulated that the unreacted $[M(cp)(CO)_3(PPh_2H)]PF_6$ in this three-component reaction mixture behaves as a very weak acid, and protonates **4** to give a very low concentration of a mixture of $[(OC)_2(cp)MH(\mu\text{-}PPh_2)Pt(CO)(PPh_3)]^+$ [cation of **12a** (M = Mo) or **13b** (M = W)] and the metallaphosphine $[M(cp)(CO)_3(PPh_2)]$ **2** (Scheme 2). The metallaphosphine exchanges with the PPh_3 ligand in $[PtH(PPh_3)_3]PF_6$ **5** producing the cation $[(OC)_3(cp)M(\mu\text{-}PPh_2)PtH(PPh_3)_2]^+$ **7** and free PPh_3 [steps (vii) and (viii)]. The cation of **12a** or **13b** reacts very quickly, step (ix), with the liberated PPh_3, with loss of carbon monoxide, to produce the final product $[(OC)_2(cp)M(\mu\text{-}H)(\mu\text{-}PPh_2)Pt(PPh_3)_2]PF_6$ **8**. It is proposed that the cation **7** rearranges with CO loss to the final product **8** *via* the intermediates **18** and **14** [steps (x)–(xii)]. This sequence of reactions is very similar to that observed in the conversion of $[(OC)_5M(\mu\text{-}PPh_2)PtH(PPh_3)_2]$ into $[(OC)_4M(\mu\text{-}H)(\mu\text{-}PPh_2)Pt(PPh_3)_2]$ (M = Cr, Mo or W).[1] Support for an additional route to $[(OC)_2(cp)M(\mu\text{-}H)(\mu\text{-}PPh_2)Pt(PPh_3)_2]PF_6$ **8** not necessarily involving $[(OC)_2(cp)M(\mu\text{-}PPh_2)Pt(CO)(PPh_3)]$ comes from ^1H NMR monitoring of the first 10 min of the reaction of **1** with $[Pt(C_2H_4)(PPh_3)_2]$ (1:1 ratio). Besides the resonances associated with the approximately equimolar mixture of **1**, **4** and **5**, weak hydrido resonances assignable to **8**

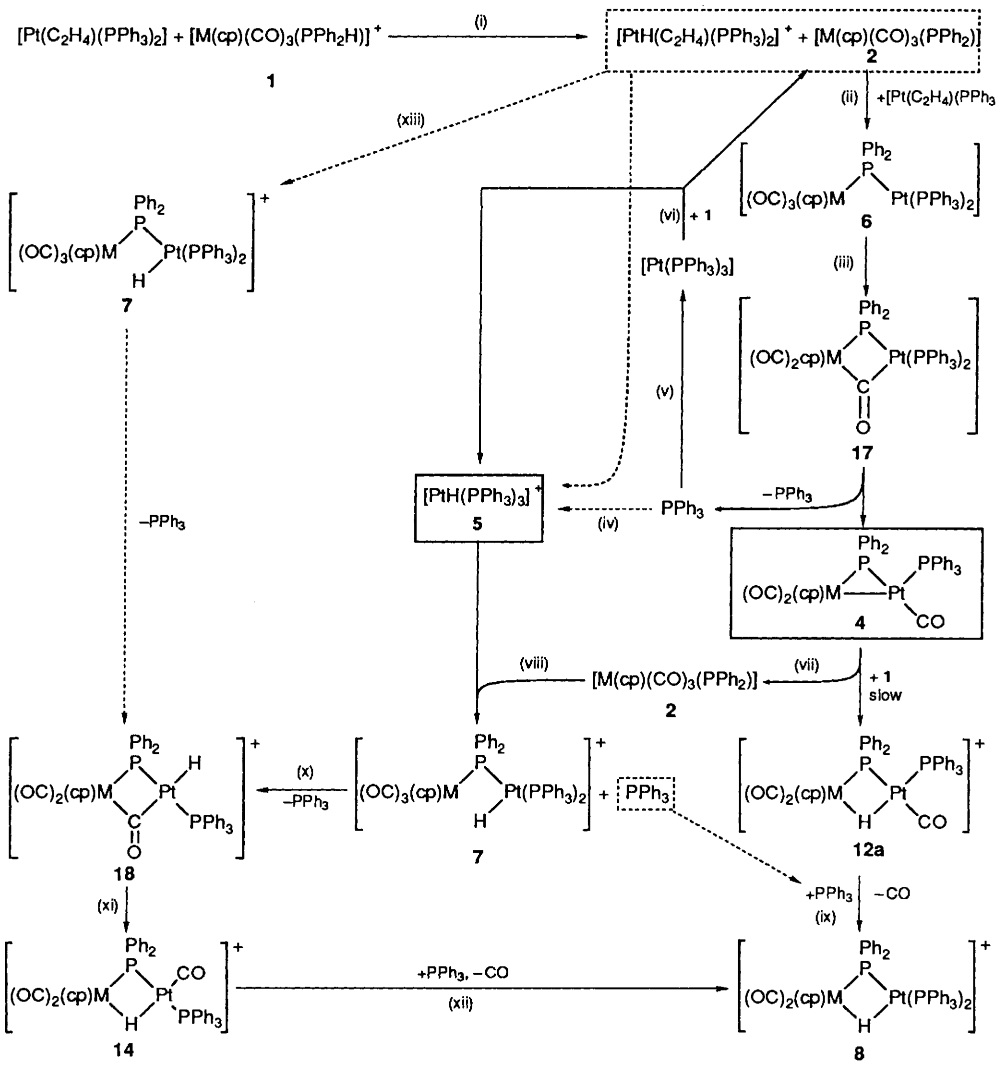

Scheme 2 Postulated pathways for the reaction of $[M(cp)(CO)_3(PPh_2H)]PF_6$ with $[Pt(C_2H_4)(PPh_3)_2]$. Complexes **4** and **5** are kinetic products [and final products of a 1:2 (M:Pt) reaction stoichiometry]; **8** is the thermodynamic product of a 1:1 reaction stoichiometry

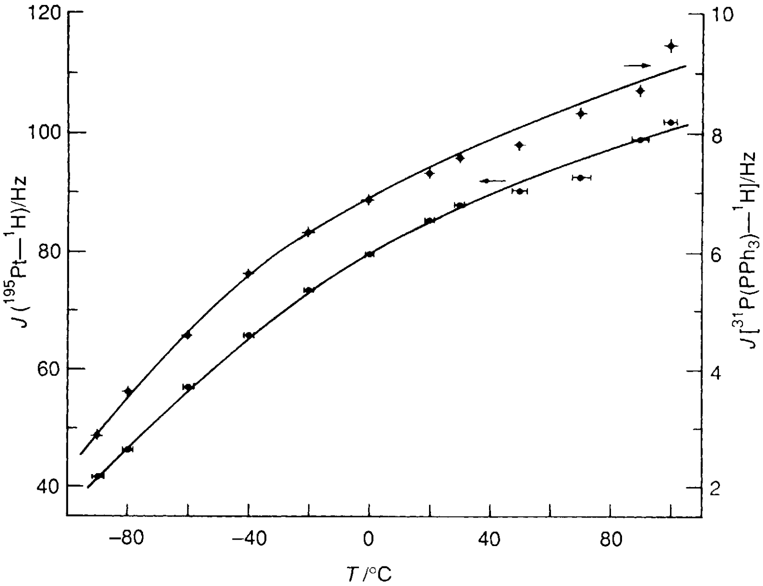

Fig. 4 Variation of the platinum-195–hydride and phosphorus-31 (PPh$_3$)–hydride coupling constants for $[(OC)_2(cp)WH(\mu\text{-}PPh_2)Pt(CO)(PPh_3)]BF_4$ in CD_2Cl_2 with temperature. The data points from 50 to 100 °C were recorded in $C_2D_4Cl_2$

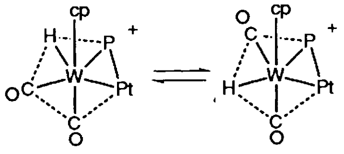

Scheme 3

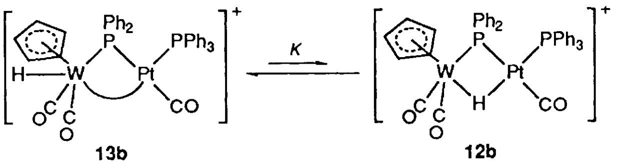

Scheme 4

Table 4 Selected bond lengths (Å) and angles (°) for [(OC)$_2$(cp)W(μ-PPh$_2$)Pt(CO)(PPh$_3$)] **4b**

	Molecule 1	Molecule 2
Pt–W	2.810(1)	2.809(1)
Pt–P(1)	2.315(2)	2.312(3)
Pt–P(2)	2.299(3)	2.287(3)
Pt–C(1)	1.838(14)	1.848(13)
W–P(2)	2.379(3)	2.377(3)
W–C(2)	1.909(12)	1.896(11)
W–C(3)	1.953(12)	1.906(13)
W–C$_t$*	1.995	1.996
W–Pt–P(1)	165.60(7)	159.97(7)
W–Pt–P(2)	54.41(6)	54.46(6)
W–Pt–C(1)	89.0(4)	93.1(4)
P(1)–Pt–P(2)	111.74(9)	105.53(9)
P(1)–Pt–C(1)	104.6(4)	107.0(4)
P(2)–Pt–C(1)	143.3(4)	147.4(4)
Pt–W–P(2)	51.78(6)	51.50(7)
Pt–W–C(2)	81.1(4)	78.1(3)
Pt–W–C(3)	122.0(3)	125.0(4)
Pt–W–C$_t$	117.2	116.9
P(2)–W–C(2)	106.3(4)	105.5(3)
P(2)–W–C(3)	80.6(3)	85.1(4)
P(2)–W–C$_t$	130.2	130.2
C(2)–W–C(3)	83.5(5)	84.5(5)
C(2)–W–C$_t$	120.5	119.7
C(3)–W–C$_t$	118.8	117.2
Pt–C(1)–O(1)	175(1)	173(1)
Pt–P(1)–C(11)	118.1(3)	115.8(4)
Pt–P(1)–C(21)	112.4(4)	116.4(3)
Pt–P(2)–W	73.81(8)	74.04(8)

* C$_t$ is the centroid of the cp ligand.

are also observed (*ca.* 5% relative to hydrido resonances of **5**. The rate of formation of **8** in the first 10 min is much faster than the subsequent **1**, **4**, **5** to **8** reaction [equation (4)] and implies a different minor pathway for the formation **8** [*i.e.* steps (xiii), (x), (xi), (xii), Scheme 2]. The reaction sequences (Scheme 2) are similar to the proton and CO transfer pathways observed in the formation of [(ON)H(cp)Re(μ-PR$_2$)Pt(PPh$_3$)$_2$]BPh$_4$ from the reaction of [Re(cp)(CO)(NO)(PR$_2$H)]BPh$_4$ with [Pt(PPh$_3$)$_4$].[2] The factors that determine the preference for P–H oxidative addition to Pt^0 [*e.g.* (xiii), Scheme 2] or for P–H deprotonation [*e.g.* (ii) Scheme 2] have been discussed elsewhere.[5]

Variable-temperature ^{1}H *NMR Studies of* [(OC)$_2$H(cp)W(μ-PPh$_2$)Pt(CO)(PPh$_3$)]BF$_4$ **13b**.—The ^{1}H NMR spectrum of the hydride ligand of complex **13b** (CD$_2$Cl$_2$ or C$_2$D$_4$Cl$_2$) exhibited an unusual temperature dependence (Fig. 3). On lowering the temperature to −90 °C $^1J(^{195}\text{Pt}-^1\text{H})$ and $^3J(^{31}\text{P}-^1\text{H})$ decrease (see Fig. 4) whilst $^2J(^{31}\text{P}_\mu-^1\text{H})$ 46 Hz and $^1J(^{183}\text{W}-^1\text{H})$ 42 Hz remain constant, and δ(H) shifts slightly. The data suggest a rapid equilibrium exchange process involving two or more isomers with isomer ratios changing with temperature. No single isomer was 'frozen out' even at −90 °C. One possibility, based on isomerism in a pseudo-pentagonal-pyramidal structure, is illustrated in Scheme 3. This postulated mechanism is similar to the observed rapid *cis* $\rightleftharpoons$ *trans* equilibrium process observed in [W(cp)H(CO)$_2$(PPh$_3$)] complexes.[22] However the invariance of $^2J(^{31}\text{P}_\mu-^1\text{H})$ to temperature is not consistent with this process {N.B. for [W(cp)H(CO)$_2$(PPh$_3$)] $^2J(^{31}\text{P}-^1\text{H})$ changes from *ca.* 20 (*cis* isomer) to *ca.* 65 Hz (*trans* isomer)}.[21] A more probable mechanism involves a rapid equilibration of the terminal hydride [(OC)$_2$H(cp)W(μ-PPh$_2$)Pt(CO)(PPh$_3$)]BF$_4$ **13b** with a small amount of the hydride-bridged structure [(OC)$_2$(cp)W(μ-H)(μ-PPh$_2$)Pt(CO)(PPh$_3$)]BF$_4$ **12b** (Scheme 4), with the terminal hydride, **13b**, being the preferred low-temperature structure. The invariance of $^1J(^{183}\text{W}-^1\text{H})$ observed here with respect to terminal and bridge co-ordination modes (Table 2) has been commented on for the system [{W(cp)H(NO)}$_2$(μ-H)$_2$].[23] A similar rapid terminal hydride $\rightleftharpoons$ bridge hydride equilibration has been observed in the 'FePt' system [(OC)$_3$HFe(μ-PR$_2$)Pt(PR'$_3$)$_2$] $\rightleftharpoons$ [(OC)$_3$Fe(μ-H)(μ-PR$_2$)Pt(PR'$_3$)$_2$] (R' = Ph; R = C$_6$H$_{11}$, Ph or Pr^n).[4] Whilst a limiting low-temperature value of $^2J(^{195}\text{Pt}-^1\text{H})$ assignable to [(OC)$_2$H(cp)W(μ-PPh$_2$)Pt(CO)(PPh$_3$)]BF$_4$ was not obtained [*i.e.* $^2J(^{195}\text{Pt}-^1\text{H})$ was still decreasing at −90 °C] a reasonable estimate is *ca.* 16 Hz [based on the observed $^2J(^{195}\text{Pt}-^1\text{H})$ of 15.5–16.5 for the structural analogues [(OC)$_3$HFe(μ-PR$_2$)Pt(CO){P(C$_6$H$_{11}$)$_3$}] (R = Ph, Pr^n or C$_6$H$_{11}$; *cis* P-donor ligands).[24] A suitable estimate for $^2J(^{195}\text{Pt}-^1\text{H}_\mu)$ in [(OC)$_2$(cp)W(μ-H)(μ-PPh$_2$)Pt(CO)(PPh$_3$)]-BF$_4$ **12b** is 520 Hz {N.B. $^1J(^{195}\text{Pt}-^1\text{H}_\mu)$ for the molybdenum analogue **12a** is 520 Hz and $^1J(^{195}\text{Pt}-^1\text{H}_\mu)$ for *trans*-[(OC)$_2$(cp)M(μ-H)(μ-PPh$_2$)Pt(CO)(PPh$_3$)]BF$_4$ **14** is essentially the same for M = Mo or W}. Using these values the relative ratios of **13b**:**12b** and hence K (Scheme 4) can be estimated from the observed $^1J(^{195}\text{Pt}-^1\text{H})$ data {N.B. $J(^{195}\text{Pt}-^1\text{H})(\text{obs.}) = 16x + (1 - x)520$, where x = mol fraction of **13b**; $K = [\mathbf{12b}]/[\mathbf{13b}] = (1 - x)/x$}. A linear plot of log K *vs.* $1/T$ gives $\Delta H = 18.4$ kJ mol^{-1} and $\Delta S = 7.5$ J K^{-1} mol^{-1}. The observation that the bridged hydrido form **12b** is preferred at high-temperature contrasts with the system [(OC)$_3$HFe(μ-PPh$_2$)Pt(PPh$_3$)$_2$] $\rightleftharpoons$ [(OC)$_3$Fe(μ-H)(μ-PPh$_2$)Pt(PPh$_3$)$_2$][4] and with bridge $\rightleftharpoons$ terminal rearrangements of carbonyl ligands in [Co$_2$(CO)$_8$][25] where the terminal bonding mode is preferred at high temperature. The ^{1}H NMR spectrum (hydride region) of the hydrido-bridged molybdenum system [(OC)$_2$(cp)Mo(μ-H)(μ-PPh$_2$)Pt(CO)(PPh$_3$)]BF$_4$ **12a** is invariant on lowering the temperature (*i.e.* no formation of a molybdenum analogue of **13b**, even at −90 °C).

Protonation Site Preference in Compound **4**.—Thermodynamic preference for protonation at W in compound **4b** to give [(OC)$_2$H(cp)W(μ-PPh$_2$)Pt(CO)(PPh$_3$)]BF$_4$ **13b** in contrast to protonation of the Mo–Pt bond in **4a** to give [(OC)$_2$(cp)Mo(μ-H)(μ-PPh$_2$)Pt(CO)(PPh$_3$)]BF$_4$ **12a** can probably be related to (*i*) the greater bond strength of third-row (W) *vs.* second-row (Mo) M–H bonds,[20] (*ii*) the greater ease of oxidation at W *vs.* Mo, and (*iii*) the relative ease of reduction at Pt. This can be illustrated by a comparison of some possible bonding representations for metal–metal bond protonation [*e.g.* Fig. 5 (*a*)–(*c*)] with the representations (*d*) and (*e*) for protonation at the metal centre. Features (*i*)–(*iii*) would favour the terminal hydrido cation representation (*e*). The lower ν(CO) (Pt) and higher ν(CO) (W) observed for the terminal hydride **13b** *vs.* corresponding data for the hydrido-bridged molybdenum complex **12a** (Table 2) are consistent with this view [N.B. for **4a** and **4b** and **14a** and **14b** ν(CO) (Pt) are essentially the same (Mo *vs.* W) whilst ν(CO) (M) are lower for M = W *vs.* Mo in contrast to **13b**/**12a**]. Other systems observed

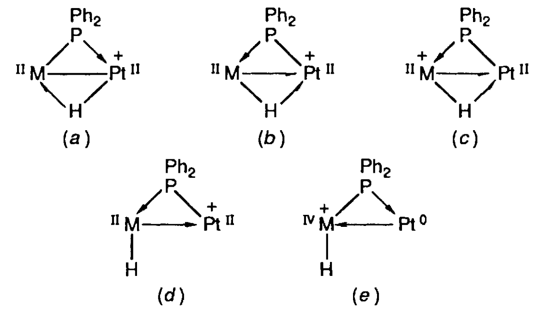

Fig. 5 Possible bonding representations for bridging and terminal 'MPt' hydrides

to date in which a terminal hydrido metal–metal bonded structure is thermodynamically preferred to a μ-hydrido structure are $[(ON)H(cp)Re(\mu\text{-}PR_2)Pt(CO)(PPh_3)]^{+}$,[2] $[(OC)_3HFe(\mu\text{-}PR_2)Pt(CO)\{P(C_6H_{11})_3\}]$,[24] $[(OC)_3HFe(\mu\text{-}PPh_2)Pt\{P(OPh)_3\}_2]$[4] (the PEt_3 analogue has a μ-hydrido structure), $[(OC)_3HRu(\mu\text{-}PPh_2)Pt(PPh_3)_2]$[24] and $[(OC)_3HRu(\mu\text{-}PPh_2)Pt(CO)(PPh_3)]$.[24] The terminal hydrido structure is favoured by W > Mo and Ru > Fe [consistent with (*i*) above]. The presence of a CO on Pt also favours the terminal hydride structure [consistent with (*iii*) above] and to date the structural arrangement of the '$(\mu\text{-}PR_2)Pt(CO)(PR_3)$' unit has the PR_3 ligand *cis* to the $\mu\text{-}PR_2$ group {even for $P(C_6H_{11})_3$ as observed in $[(OC)_3HFe\{\mu\text{-}P(C_6H_{11})_2\}Pt(CO)\{P(C_6H_{11})_3\}]$}.[24] This indicates that the observed stereochemistry at Pt is governed by platinum-ligand bonding requirements rather than steric factors. The observed stereochemistry has CO *trans* to $\mu\text{-}PR_2$ (a good σ donor).

The Molecular Structure of $[(OC)_2(cp)W(\mu\text{-}PPh_2)Pt(CO)(PPh_3)]$ **4b**.—The asymmetric unit of compound **4b** contains two independent molecules related by a pseudo B centre. The ORTEP views of the two molecules (Fig. 1) indicate that the configurations of the two W atoms are opposite and that the molecules differ in the conformations of the phosphine ligands. Notably in molecule 2 the pairs of phenyl rings (1,4) and (3,5) are closer to being parallel than the corresponding pairs of rings in molecule 1. This arrangement results in a P(1)–Pt–P(2) bond angle of 105.53(9)° which is significantly smaller than the corresponding angle in molecule 1 of 111.74(9)° (Table 4). Corresponding W–Pt–Cl angles are then slightly smaller by 4.1 and 2.4° for molecule 1. Additionally the Pt–P(2) bond is marginally shorter in molecule 2 [2.287(3) *vs.* 2.299(3) Å] and there is significantly more asymmetry between the C–P(1)–C bond angles for the PPh_3 ligand in this molecule. Similar small differences are observed at the tungsten centres in the two molecules. Recently reported compounds containing structural features similar to **4b** are $[(OC)_2(cp)Mo\{\mu\text{-}P(C_6H_{11})_2\}Pd\{P(C_6H_{11})_2H\}_2]$ and $[(OC)_4Mn\{\mu\text{-}P(C_6H_{11})_2\}Pd\{P(C_6H_{11})_2H\}_2]$.[25]

Experimental

All manipulations were carried out under an atmosphere of dry N_2, using dry, degassed solvents. Infrared spectra (as CH_2Cl_2 solutions) were recorded on a Nicolet 10DX spectrometer, ^1H and $^{31}P\text{-}\{^1H\}$ NMR spectra (CD_2Cl_2) on a Varian XL 200 spectrometer, referenced to $SiMe_4$ and 85% H_3PO_4 respectively. Elemental analyses were performed by Canadian Microanalytical Laboratories, Vancouver, B.C.

Preparation of Complexes.—Representative examples are given for the molybdenum–platinum dimers and precursors. The tungsten–platinum dimers were prepared following identical procedures.

$[Mo(cp)(CO)_3(PPh_2H)]PF_6$ **1a**. This compound was synthesised using the procedure of Treichel *et al.*[13] with minor modifications. In a typical reaction $[Mo(cp)(CO)_3Cl]$ (4.03 g, 14.4 mmol) and $AlCl_3$ (2.38 g, 17.8 mmol) were stirred in dry benzene (180 cm^3) for 30 min at 25 °C. Then freshly distilled PPh_2H (2.5 cm^3, 14.4 mmol) was added and the reaction stirred overnight. The solvent was removed *in vacuo* and the residue extracted twice with distilled water (50 cm^3). The water extracts were filtered directly into a saturated aqueous NH_4PF_6 solution (300 cm^3). A yellow solid precipitated immediately on contact with the aqueous ammonium hexafluorophosphate solution. The extraction was repeated twice more using 25% acetone–water (50 cm^3). The yellow solid was then collected by gravity filtration and dried (24 h in a vacuum desiccator kept in the dark). Yield of compound **1a** 3.98 g (6.9 mmol, 48%).

$[(OC)_2(cp)Mo(\mu\text{-}PPh_2)Pt(CO)(PPh_3)]$ **4a**. The compound $[Pt(C_2H_4)(PPh_3)_2]$[26] (2.66 g, 3.56 mmol) was dissolved in dry CH_2Cl_2 (100 cm^3). Complex **1a** (1.03 g, 1.78 mmol) was dissolved in dry CH_2Cl_2 (50 cm^3) and added slowly, dropwise with stirring, to the platinum solution over a period of 30 min. The mixture was stirred for an additional 30 min at 20 °C and the solvent removed *in vacuo*. The red residue was extracted with hot, dry benzene (25 cm^3). Out of the benzene precipitated off-white crystals of $[PtH(PPh_3)_3]PF_6$ **5** (1.77 g, 1.57 mmol, 88%). The solvent was removed from the mother-liquor and the red residue recrystallized from a minimum of acetone to yield 1.25 g (1.41 mmol, 79%) of red crystalline $[(OC)_2(cp)Mo(\mu\text{-}PPh_2)Pt(CO)(PPh_3)]$ [Found (Calc. for $C_{32}H_{30}MoO_3P_2Pt$ **4a**): C, 51.3 (51.4); H, 3.50 (3.40). Found (Calc. for $C_{32}H_{30}O_3P_2PtW$ **4b**): C, 47.0 (46.8); H, 3.05 (3.10)%].

$[(OC)_2(cp)Mo(\mu\text{-}H)(\mu\text{-}PPh_2)Pt(PPh_3)_2]PF_6$, **8a**. *Method* (*a*). The compound $[Mo(cp)(CO)_3(PPh_2H)]PF_6$ **1a** (0.280 g, 0.485 mmol) was dissolved in dry CH_2Cl_2 (50 cm^3). While stirring, $[Pt(C_2H_4)(PPh_3)_2]$ (0.365, 0.489 mmol) was added over 15 min. The bright yellow reaction mixture turned slowly to yellow-orange over 16 h. Removal of the solvent *in vacuo* and recrystallization from CH_2Cl_2–hexanes gave $[(OC)_2(cp)Mo(\mu\text{-}H)(\mu\text{-}PPh_2)Pt(PPh_3)_2]PF_6$ (0.50 g, 0.402 mmol, 83%) as a yellow crystalline solid [Found (Calc. for $C_{55}H_{46}F_6MoO_2P_4Pt$ **8a**): C, 51.5 (52.1); H, 3.80 (3.65); P, 10.0 (9.8). Found (Calc. for $C_{55}H_{46}F_6O_2P_4PtW$ **8b**): C, 47.5 (48.7); H, 3.40 (3.40); P, 8.9 (9.1)%].

Method (*b*). The compound $[(OC)_2(cp)Mo(\mu\text{-}H)(\mu\text{-}PPh_2)Pt(PPh_3)_2]BF_4$ can be isolated in 80–90% yield by the reaction of $[(OC)_2(cp)Mo(\mu\text{-}PPh_2)Pt(PPh_3)_2]$ **9** with 1 equivalent of $HBF_4\cdot OEt_2$ in CH_2Cl_2.

$[(OC)_2(cp)Mo(\mu\text{-}PPh_2)Pt(dppe)]$ **10**. The compound $[(OC)_2(cp)Mo(PPh_2)Pt(CO)(PPh_3)]$ (0.133 g, 0.150 mmol) was dissolved in dry CH_2Cl_2 (25 cm^3) and 1,2-bis(diphenylphosphino)ethane (dppe) (0.062 g, 0.155 mmol) added. The reaction mixture was stirred for 30 min at 20 °C and the solvent removed *in vacuo*. The residue was washed with three portions (10 cm^3) of hexanes at 50 °C to remove free PPh_3. The orange-red residue was then recrystallized from CH_2Cl_2–hexanes to yield 0.140 g (0.141 mmol, 94%) of $[(OC)_2(cp)Mo(\mu\text{-}PPh_2)Pt(dppe)]$ **10** as an orange-red powder (not completely PPh_3 free).

$[(OC)_2(cp)Mo(\mu\text{-}PPh_2)Pt(PPh_3)_2]$ **9a**. In a typical reaction $[(OC)_2(cp)Mo(\mu\text{-}PPh_2)Pt(CO)(PPh_3)]$ **4a** (0.109 g, 0.123 mmol) and PPh_3 (0.324 g, 0.124 mmol) were refluxed in dry benzene for 30 min. The solvent was removed *in vacuo* and the red-orange residue recrystallized from CH_2Cl_2–hexanes to yield orange crystals of $[(OC)_2(cp)Mo(\mu\text{-}PPh_2)Pt(PPh_3)_2]$ **9a** (0.122 g, 0.109 mmol, 89%) [Found (Calc. for $C_{55}H_{45}MoO_2P_3Pt$ **9a**): C, 55.2 (55.7); H, 3.90 (3.90). Found (Calc. for $C_{55}H_{45}O_2P_3PtW$ **9b**): C, 50.7 (50.8); H, 3.40 (3.60)%].

$[(OC)_2(cp)Mo(\mu\text{-}H)(\mu\text{-}PPh_2)Pt(dppe)]BF_4$ **11a**. A solution of $HBF_4\cdot OEt_2$ (0.26 cm^3, 0.308 g, 1.90 mmol) in dry Et_2O (4.0

cm^3) (*i.e.* 0.467 mol dm^{-3}) was prepared; 0.055 cm^3 (0.926 mmol) of the solution was added to a solution of [(OC)$_2$(cp)Mo(μ-PPh$_2$)Pt(dppe)] **10** (0.026 g, 0.026 mmol) in dry CH$_2$Cl$_2$ (10 cm^3). The solution went from bright orange to bright yellow immediately upon addition of the acid. The solvent was removed *in vacuo* and the residue dried for 30 min under high vacuum at 25 °C. Yield of [(OC)$_2$(cp)Mo(μ-H)(μ-PPh$_2$)Pt(dppe)]BF$_4$ was 0.027 g (0.025 mmol, 97%).

[(OC)$_2$(cp)Mo(μ-H)(μ-PPh$_2$)Pt(CO)(PPh$_3$)]BF$_4$ **12a**. A solution of HBF$_4$·OEt$_2$ (0.130 cm^3, 0.952 mmol) in dry Et$_2$O (4.0 cm^3) (*i.e.* 0.238 mol dm^{-3}) was prepared. The compound [(OC)$_2$(cp)Mo(μ-PPh$_2$)Pt(CO)(PPh$_3$)] **4a** (0.084 g, 0.095 mmol) was dissolved in dry, degassed CH$_2$Cl$_2$ (20 cm^3) and 0.40 cm^3 of the HBF$_4$–Et$_2$O solution added. The solvent was removed *in vacuo* and the white-yellow residue dried *in vacuo* for 2 h. The residue was redissolved in dry, degassed CD$_2$Cl$_2$ (0.75 cm^3) transferred to a thick-walled 5 mm NMR tube and the NMR tube sealed *in vacuo*. The ^{1}H and ^{31}P-{^{1}H} NMR spectra were recorded. The compound *trans*-[(OC)$_2$(cp)Mo(μ-H)(μ-PPh$_2$)Pt(PPh$_3$)(CO)]BF$_4$ **14a** was characterized by ^{1}H and ^{31}P-{^{1}H} NMR monitoring of the sealed NMR sample from the preparation of complex **12a** which had been subsequently kept at 25 °C for 24 h to ensure complete rearrangement of **12a** to **14a**.

[(OC)$_2$(cp)Mo(μ-H)(μ-PPh$_2$)PtCl(PPh$_3$)] **15a**. To a solution of [(OC)$_2$(cp)Mo(μ-PPh$_2$)Pt(CO)(PPh$_3$)] **4a** (0.064 g, 0.071 mmol) in dry, degassed CH$_2$Cl$_2$ (25 cm^3) was added a 0.46 mol dm^{-3} solution of HCl (0.175 cm^3, 0.080 mmol) in benzene. A small sample (0.5 cm^3) was removed to record an infrared spectrum. The solvent was then removed *in vacuo* from the remainder and the orange residue dried at 25 °C *in vacuo* for 2 h. It was redissolved in dry, degassed CD$_2$Cl$_2$ (0.75 cm^3), transferred to a thick-walled 5 mm NMR tube and sealed *in vacuo*. The ^{1}H and ^{31}P-{^{1}H} NMR spectra were recorded.

[(OC)$_2$(cp)Mo(μ-H)(μ-PPh$_2$)PtCl(PPh$_3$)] **16a**. This compound was characterized by ^{1}H and ^{31}P-{^{1}H} NMR monitoring of the sealed tube from the preparation of complex **15a**, after the sample had been kept at 25 °C for 7 d to allow complete rearrangement to **16a**.

X-Ray Crystallography.—Structural data for [(OC)$_2$(cp)W(μ-PPh$_2$)Pt(CO)(PPh$_3$)] **4b** are available on the Cambridge Crystallographic Data base as ref. code DAPPOZ. Requests citing ref. 10, should be directed to the Cambridge Crystallographic Data Centre, University Chemical Laboratory, Lensfield Road, Cambridge CB2 1EW.

Acknowledgements

We thank the Natural Sciences and Engineering Research Council of Canada for financial support.

References

1 J. Powell, M. R. Gregg and J. F. Sawyer, *Inorg. Chem.*, 1989, **28**, 4451.
2 J. Powell, J. F. Sawyer and M. V. R. Stainer, *Inorg. Chem.*, 1989, **28**, 4461.
3 J. Schwald and P. Peringer, *J. Organomet. Chem.*, 1987, **212**, C51.
4 J. Powell, M. R. Gregg and J. F. Sawyer, *J. Chem. Soc., Chem. Commun.*, 1987, 1029.
5 J. Powell, E. Fuchs, M. R. Gregg, J. Phillips and M. V. R. Stainer, *Organometallics*, 1990, **9**, 387.
6 J. Powell, J. C. Brewer, G. Gulia and J. F. Sawyer, *Inorg. Chem.*, 1989, **28**, 4470.
7 J. Powell, D. Fuchs and J. F. Sawyer, *Organometallics*, 1990, **9**, 1722.
8 J. Powell, M. R. Gregg and J. F. Sawyer, *Inorg. Chem.*, 1988, **27**, 4521.
9 J. Powell and M. R. Gregg, *J. Organomet. Chem.*, 1988, **356**, C61.
10 J. Powell, J. F. Sawyer and S. J. Smith, *J. Chem. Soc., Chem. Commun.*, 1985, 1312.
11 T. Blum, P. Braunstein, A. Tiripicchio and M. Tiripicchio, *New J. Chem.*, 1988, **12**, 539.
12 R. B. King and F. G. A. Stone, *Inorg. Synth.*, 1963, **7**, 99; N. W. Hoffman, *Inorg. Chim. Acta*, 1984, **88**, 59.
13 P. M. Triechel, W. K. Dean and W. M. Douglas, *J. Organomet. Chem.*, 1972, **42**, 145.
14 W. Malisch, R. Maisch, I. J. Colquhoun and W. J. McFarlane, *J. Organomet. Chem.*, 1981, **220**, C1.
15 W. E. Buhro, S. Georgion, J. P. Hutchinson and J. A. Gladysz, *J. Am. Chem. Soc.*, 1985, **107**, 3346.
16 R. W. Caputo, D. K. Mak, R. D. Willet, S. G. Roundhill and D. M. Roundhill, *Acta Crystallogr., Sect. B*, 1977, **33**, 215.
17 T. W. Dingle and K. Dixon, *Inorg. Chem.*, 1974, **13**, 847.
18 A. R. Manning, *J. Chem. Soc. A*, 1967, 1984.
19 F. A. Cotton and C. M. Lukehart, *J. Am. Chem. Soc.*, 1971, **93**, 2672.
20 D. S. Moore and S. D. Robinson, *Chem. Soc. Rev.*, 1983, **12**, 415.
21 D. J. Darensbourg, *Adv. Organomet. Chem.*, 1982, **21**, 112.
22 P. Kalck, R. Prince, R. Poilblanc and J. Russel, *J. Organomet. Chem.*, 1970, **24**, 445.
23 P. Legzdins, J. T. Martin, F. W. B. Einstein and A. C. Willis, *J. Am. Chem. Soc.*, 1986, **108**, 7971.
24 J. Powell and M. R. Gregg, unpublished work.
25 P. Braunstein, E. de Jesus, A. Tiripicchio and M. Tiripicchio Camellini, *J. Organomet. Chem.*, 1989, **368**, C5.
26 D. M. Blake and D. M. Roundhill, *Inorg. Synth.*, 1978, **18**, 120.

Received 7th April 1992; *Paper* 2/01841A